



Geophysical Research Letters*

RESEARCH LETTER

10.1029/2021GL095354

Key Points:

- On average 30% of the year the soil below global snowpack is unfrozen
- Seasonal evolution of the areas of unfrozen soil below snowpack is not synchronous with snow cover extent
- Basal snowpack melting could have increased in a warming climate

Supporting Information:

Supporting Information may be found in the online version of this article.

Correspondence to:

L. Gao, gaoxx996@umn.edu

Citation:

Gao, L., Ebtehaj, A., Cohen, J., & Wigneron, J.-P. (2022). Variability and changes of unfrozen soils below snowpack. *Geophysical Research Letters*, 49, e2021GL095354. https://doi.org/10.1029/2021GL095354

Received 20 JUL 2021 Accepted 31 JAN 2022

Author Contributions:

Conceptualization: Lun Gao, Ardeshir Ebtehaj

Formal analysis: Lun Gao, Ardeshir Ebtehaj, Judah Cohen, Jean-Pierre Wigneron

Funding acquisition: Lun Gao, Ardeshir Ebtehaj

Supervision: Ardeshir Ebtehaj Writing – original draft: Lun Gao, Ardeshir Ebtehai

Writing – review & editing: Lun Gao, Ardeshir Ebtehaj, Judah Cohen, Jean-Pierre Wigneron

© 2022. American Geophysical Union. All Rights Reserved.

Variability and Changes of Unfrozen Soils Below Snowpack

Lun Gao¹, Ardeshir Ebtehaj¹, Judah Cohen^{2,3}, and Jean-Pierre Wigneron⁴

¹Department of Civil, Environmental, and Geo- Engineering, Saint Anthony Falls Laboratory, University of Minnesota, Minneapolis, MN, USA, ²Atmospheric and Environmental Research, Inc., Lexington, MA, USA, ³Department of Civil and Environmental Engineering, Massachusetts Institute of Technology, Cambridge, MA, USA, ⁴INRA, UMR1391 ISPA, Bordeaux, France

Abstract Using four reanalysis data sets and ground-based observations, this paper uncovers that on average, 30% of the time, Northern Hemisphere snow cover experiences unfrozen bottom soil. It is demonstrated that the probability of occurrence of unfrozen soils is correlated with the snow types and is maximum over the ephemeral followed by the maritime and prairie snow. The results based on reanalysis data unveil that the seasonal evolution of the unfrozen soil areas is not synchronous with the snow cover extent and exhibits sub-annual bi-modality with two annual maxima in April and October. Interannual trend analyses indicate that shrinkage of spring snow in the past few decades has been accompanied by an increase in the proportion of unfrozen bottom soils, more significantly over polar climate regimes dominated by the tundra and taiga snow. The findings imply that the snowpack basal melting could have increased due to global warming.

Plain Language Summary Unfrozen bottom soils below snow layers play an important role in the persistence and stability of snowpack, yet less knowledge is known about its spatial variability and seasonal evolution on a global scale. This study uncovers that, on average, around 30% of annual Northern Hemisphere's snow cover extent is over unfrozen soils with a spatial variability that is highly correlated with snow types. Specifically, unfrozen soils appear more frequently below the ephemeral followed by the maritime and prairie snow. In addition, it is demonstrated that the unfrozen soil areas exhibit different seasonal evolution from snow cover extent with two annual peaks in April and October. The results show that the areas of unfrozen soils are expanding in spring as the snow cover extent is shrinking.

1. Introduction

Snow cover has cooling effects on the climate system (Cohen & Rind, 1991; Cohen et al., 2012; Vavrus, 2007) and influences seasonal carbon balance across different biomes (Pulliainen et al., 2017; Winchell et al., 2016) by modulating the underlying soil frost depth (Iwata et al., 2010) as well as activities of snow (Dominé & Shepson, 2002; Zhu et al., 2019) and soil microbial communities (Zona et al., 2016). Meltwater of snow is critical for the functioning of the ecosystem and sustainability of socioeconomic developments (Mankin et al., 2015). Snowmelt is one of the main sources of streamflow (Barnhart et al., 2016; Nijssen et al., 2001) and groundwater recharge in headwater basins (Earman et al., 2006; Wu et al., 2020), northern forests, and cold semi-arid climates (Gray, 1970). Observational evidence (Brown & Robinson, 2011; Derksen & Brown, 2012; Déry & Brown, 2007; Robinson et al., 1993) and climate projections (Brown & Mote, 2009; Mudryk et al., 2020) suggest that the Northern Hemispheric (NH) snow has been and will continue to shrink due to global warming (Cohen, 1994; McCabe & Wolock, 2010) and changes of precipitation patterns (Karl et al., 1993; Tamang et al., 2020). Early snowmelt shifts the peak runoff to the early spring, causing water shortages for the downstream ecosystem in summer (Barnett et al., 2005).

Stability and maintenance of seasonal snowpack depend on the dynamics of its energetics (Lemke et al., 2007; Pomeroy et al., 2003). Snow largely exchanges energy and mass over its interface with the atmosphere and soil through radiative, sensible, latent, and advective heat fluxes (Pomeroy & Brun, 2001). Compared to energy exchanges with atmosphere, the ground heat flux is traditionally considered to be a small portion of the energy balance (DeWalle & Rango, 2008). However, due to its persistence, it has a significant cumulative effect on accelerating or retarding the seasonal melting processes (Pomeroy & Brun, 2001).

Numerous field studies (Blankinship et al., 2014; Boike et al., 2003; Decker et al., 2003; DeWalle & Rango, 2008; Granger & Male, 1978; Marks & Winstral, 2001; Tyler et al., 2008) indicate that the temperature at the soil-snow

GAO ET AL.



Table 1				
Specifications of MERRA-2, ERA-Interim, ERA5, and GLDAS Products				
	MERRA-2	ERA-Interim	ERA-5	GLDAS
Spatial resolution (degree)	0.5×0.625	0.25×0.25	0.25×0.25	0.25×0.25
Temporal resolution (hourly)	1	3	1	1
Number of soil layers	6	4	4	4
Top soil thickness (cm)	0 - 10	0 - 7	0 - 7	0 – 10
Time coverage	01/1 980 - 12/2 020	01/1 979 - 08/2 019	01/1 979 – 12/2 020	01/2 000 - 09/2 020

interface can be frequently above the freezing point. Diurnal and seasonal dynamics of the bottom soil temperature (ST) can alter the timing and distribution of snowmelt runoff. When the bottom soil unfreezes, there exist positive pulses of upward heat fluxes from soil to snowpack (Huang et al., 2017; Zhang, 2005). These fluxes can reach up to 850 kJ m⁻² per day (Goodrich, 1982) and melt the snowpack from the bottom. Consequently, the advective heat flux of meltwater infiltration can further warm up the upper soil layer and amplify its infiltration capacity (Williams & Smith, 1991). When the interfacial soil moisture refreezes at night, a significant amount of latent heat is released (Zhao et al., 1997), which can increase meltwater overland runoff (Mazurkiewicz et al., 2008) due to impeded infiltration over frozen soils (Iwata et al., 2010). Therefore, dynamics of bottom ST can strongly influence the present and future trends of snow cover extent (SCE) Mudryk et al. (2017).

Despite numerous field experiments, it is not yet well-understood when and where the ST below snowpack can be above 0°C. Satellite observations in the visible to microwave bands enable to retrieve the surface skin temperature (André et al., 2015; Duan et al., 2017; Holmes et al., 2009; Jiménez-Muñoz et al., 2014; Kerr et al., 1992; Mao et al., 2005; McFarland et al., 1990; Njoku & Li, 1999; Sobrino et al., 2004) but not at the soil-snowpack interface. This paper quantifies when and where the surface ST beneath the snowpack can be above the freezing point across the NH and studies the trend in spatial extent and occurrence of this phenomenon for different snowpack climatology in the past 40 years — using four reanalysis products and ground-based observations.

2. Data

The four reanalysis products used in this study are the second Modern-Era Retrospective analysis for Research and Applications (MERRA-2) (Gelaro et al., 2017) by the National Aeronautics and Space Administration (NASA), the ERA-Interim (Dee et al., 2011) and ERA5 (Hersbach et al., 2020) by the European Centre for Medium-Range Weather Forecasts (ECMWF), and the NASA's Global Land Data Assimilation System (GLDAS, version 2.1) (Rodell et al., 2004). More descriptions about land surface models of each reanalysis are provided in the Supporting Information S1.

For each reanalysis product, two land surface variables are used: top surface ST and snow depth (SD) to determine the presence or absence of snow (Table 1). To complement the analyses, we also use hourly measurements of ST and SD from the SNOwpack TELemetry (SNOTEL) network (Schaefer & Paetzold, 2001; Serreze et al., 1999) in the western United States — collected from 220 valid sites, available in the International Soil Moisture Network (ISMN) (Dorigo et al., 2011) database. Those sites with at least 5 years of measurements with good quality flags (Dorigo et al., 2013) are used in this study.

3. Methodology

For each snapshot of reanalysis data at time t, the snow cover at each pixel (i, j) is where SD is greater than 1 mm rather than zero to avoid the influence of artifacts in the treatment of snow melt. The threshold of SD is determined based on the uncertainty analysis reported in the Table S1 in the Supporting Information S1. Note that, unlike other reanalysis products, the SD in MERRA-2 is only reported over the snow-covered fraction of its grid cells (Reichle et al., 2017; Toure et al., 2018). Therefore, to present the results consistently, the MERRA2 mean SD over the entire grid cell is computed by multiplying the SD with its fraction. The snow-covered pixels with unfrozen soils are those where ST is above 0° C. The SCE for all pixels and those with unfrozen bottom soils (SCE_{ubs}) are the sum of the areas of all pixels at each snapshot. To compute the probability of occurrence

GAO ET AL. 2 of 12



of SCE_{ubs} over a time window, we first generate a binary mask $\mathbf{I}_{\text{ubs}}^{t}(i, j)$ at time t, where $\mathbf{I}_{\text{ubs}}^{t}(i, j) = 1$, when snow exists with unfrozen bottom soils and zero elsewhere. Then, the conditional probability of occurrence over a period of time T, given that the snow cover exists, is $p_{\text{ubs}}(i, j) = T^{-1} \sum_{t=1}^{T} \mathbf{I}_{\text{ubs}}^{t}(i, j)$. Five different range of probability values are considered for discussion: low (0 + 0.2), moderately low (0.2 - 0.4), moderate (0.4 - 0.6), moderately high (0.6 - 0.8) and high (0.8 - 1).

For the trend analysis, we adopt the Theil – Sen estimator (Sen, 1968; Theil, 1992), which does not rely on any parametric assumptions about the probability distribution of the data. This method is less sensitive to outliers and remains robust to skewed and heteroskedastic data (Wilcox, 2010), compared to an ordinary least squares estimator (Matoušek et al., 1998). To quantify the statistical significance of the trends, the bootstrap Mann – Kendall test (Douglas et al., 2000) is adopted, which is known to be suitable for proper detection of linear trends in a non-Gaussian sample space (Yue & Pilon, 2004). See the Supporting Information S1.

4. Results and Discussion

4.1. Spatial Variability

Seasonal variability of $p_{\rm ubs}$ (i, j) over NH for the reanalysis data are shown in Figure 1. Although there exist known uncertainties in reanalysis data (Albergel et al., 2015; Cao et al., 2020; Holmes et al., 2012; Wang et al., 2016; Yang & Zhang, 2018); we see extensive areas of unfrozen soils for more than 50% of the snowpack life cycle. Over the winter, all reanalysis products are relatively consistent, showing the areas of unfrozen bottom soil with an occurrence probability of \geq 0.5 vary from 13 (GLDAS) to 19 (MERRA-2) million km², which is equivalent to 20 – 27% of SCE. As the temperature rises, the discrepancies between the reanalysis products grow. For example, from March to May, on average, the areas associated with $p_{\rm ubs}$ (i, j) \geq 0.5 are 27, 23, 23, 14 million km² in MERRA-2, ERA-Interim, ERA5, and GLDAS, respectively. In the summer, this area expands to 23 – 37 million km² that is, 71 – 94% of SCE.

The shown classes are Ice (Ic), ephemeral (Ep), prairie (Pr), maritime (Ma), alpine (Al), taiga (Ta), and tundra (Tu).

Spatial variability of $p_{\rm ubs}$ (i,j) (Figure 1a) seems to be strikingly correlated with the snow classes (Figure 1b) as defined by Sturm et al. (1995) that discriminate the NH snow into taiga, alpine, maritime, prairie, ephemeral, and tundra — based on the snow stratigraphy and texture. Tundra snow is thin with maximum depth of 75 cm and consists of a basal layer of depth hoar overlaid by multiple wind slabs. The Taiga snow represents a moderately thick but light snowpack with maximum depth and density of 120 cm and 260 kg m⁻³, with a stratigraphy that is dominated by depth hoar covered by new snow. The alpine and maritime snows are the deepest and the most structurally complex ones, with layers of varying grain size, wetness, and ice bodies. The prairie and ephemeral snow are shallow with a depth of less than 50 cm. The prairie snow is moderately cold with substantial wind drift and frequent wind slabs while ephemeral snow consists of thin layers of new warm snow with ice layers on the top and bottom.

Figures 1a and 1c show that during the winter, $p_{\rm ubs}(i,j)$ values are maximum below the ephemeral snow followed by the maritime. The values are low over the tundra and taiga snow in Russia, Canada, and Northern Europe above 45°N as well as over the Tibetan highlands. The extension of these low probability areas over high-altitude mountains such as the Rockies and Alps is also evident. The alpine snow in Canada does not experience frequent unfrozen bottom soil, while this is not the case in Western Russian and Eastern Europe where the probability ranges from moderately low to moderate. There are moderately high to high $p_{\rm ubs}(i,j)$ values over the Southern United States, Eastern China, and Middle East. The transition from low to high probabilities over Asia is sharper than Europe and North America, perhaps because the snow type transitions sharply from tundra to prairie over Asia while in Europe and North America this transition is moderated due to the presence of more persistent alpine and maritime snow. It is important to observe that the probability is high under the ephemera snow, consistently among all reanalysis data, and in North America, this high probability even extends to the maritime snow of the Coast Mountains of Canada.

The probability of warm soil sharply increases, on average, from 0.14 to 0.46 (0.11–0.37) over the prairie (alpine) snow from winter to spring (Figures 1a and 1c). In spring, the tundra and taiga snow above the Arctic Circle do not experience frequent unfrozen soils, especially over Russia and Canada and the probability remains low

GAO ET AL. 3 of 12

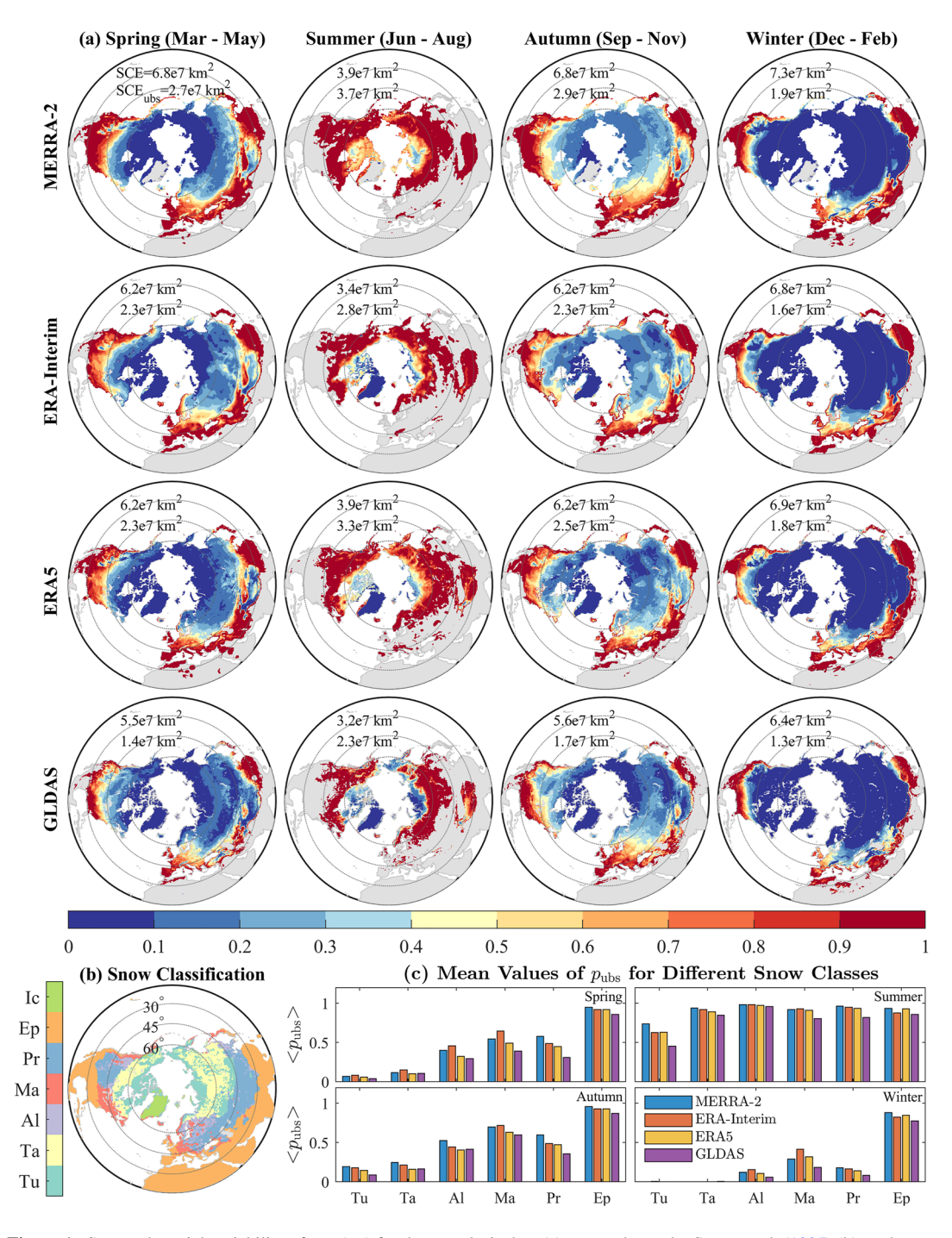


Figure 1. Seasonal spatial variability of $p_{\text{ubs}}(i, j)$ for the reanalysis data (a), snow classes by Sturm et al. (1995) (b), and spatial mean of $p_{\text{ubs}}(i, j)$ for each snow type at different seasons (c). For each season, the values of snow cover extent (SCE) and SCE_{ubs} with $p_{\text{ubs}}(i, j) \ge 0.5$ are reported on the insets, where SCE denotes the maximum seasonal snow cover extent.

above the Arctic Circle. Although, there are some noticeable inconsistencies among reanalysis products over the Scandinavian Mountains in Norway, where the snow is largely tundra in the north and maritime in the south. The probability transition from low (north) to high (south) in MERRA-2 and ERA5 is consistent with the snow class; however, it remains high (low) from north to south in ERA-Interim (GLDAS). Another example is over the Aleutian Islands in Alaska, where the probability is high in MERRA-2 but moderate in the other reanalysis datasets. Between 45 and 60°N, the taiga snow over Eastern Russia exhibits a low to moderately low probability of warm soil. However, across the western Eurasia with a mixture of alpine, prairie, and maritime snow; the probability

GAO ET AL. 4 of 12



increases to moderate and moderately high. Below 45°N, the snow type is largely prairie (maritime) over Eurasia and Western (Eastern) United States. It appears that the probability of unfrozen soil is moderately high to high regardless of the snow type in this latitudinal belt in spring. As the elevation increases, the probability decreases to moderately low for example, over the Rockies and Tibetan highlands.

In summer, snow is largely above 45° N, where p_{ubs} (i,j) values, on average, are more than 0.5 for all types. Among all reanalysis products, the probability is moderately high to high outside the Arctic Circle, even over the Tibetan highlands (Figures 1a and 1c). However, in MERRA-2, moderate and moderately high probable areas extend even to tundra, while above 60° N, the probability remains below moderately low in other data sets, especially over the Taymyr Peninsula and the Arctic Archipelago. Transitioning to the autumn, the pattern of spatial probabilities becomes similar to the spring; however, warm soil is slightly more probable below the tundra and taiga snow. Within $45-60^{\circ}$ N, the probability increases from east to west over Eurasia when the dominant snow type transitions from tundra and taiga in the Russian Far East to alpine, prairie, and maritime in western Europe. In MERRA-2, the probability remains high and does not seem to be correlated with the snow type over the United States. However, in the other three products, it is often lower over the Rockies. The bottom soil of maritime snow in this belt is consistently warm among all data sets near the coastlines. As previously explained, reanalysis data are subject to model errors. The questions are — what is the accuracy of reanalysis data in modeling the ST below the snowpack? Can we obtain the same order of p_{ubs} (i,j) using ground-based data?

To answer the first question we need to compare the ground-based observations and reanalysis data. However, Cao et al. (2020) found that ERA5 has systematic warm and cold biases, from polar to middle latitudes, ranging from -1.6 to 2.09° C at the surface soil layer. Guided by this finding, we delineate and report the areas with p_{ubs} (i, j) < 0.5 (Figure S1 and Table S2 in the Supporting Information S1), considering that the freezing point exhibits uncertainty range $\pm 1-2^{\circ}$ C.

To address the second question, we focus on hourly measurements of surface ST and SD from the SNOTEL network across the Western United States and Alaska, using available high-quality surface ST below snowpack with a sample size of 10,000-100,000 at each station. The results confirm that the probability of warm soil varies across different snow types and is at the same order of magnitude as inferred from the reanalysis data (Figure 2a). Annual $p_{\rm ubs}$ is typically less than 0.4 over Alaska where tundra and taiga are the dominant snow types and increases noticeably over the southern coastlines of Alaska with maritime snow. The probability values in the Western United States, with maritime and ephemeral snow, are moderately high or high, consistently among all stations. However, among those with the alpine and prairie snow, a great deal of heterogeneity is observed due to the impacts of complex topography on snow energetics.

Figure 2b shows the probability density function (PDF) of ST for different snow types + obtained by collapsing the measurements of all available stations over each snow class. The probability of unfrozen soil is 0.19 and 0.31 over tundra and taiga, where the ST can decrease to -15° C. By contrast, on average, it increases to more than 0.6 for alpine (0.65), maritime (0.75), prairie (0.7), and ephemeral (0.85) snow, where the ST barely drops below -2° C. Time series of bottom ST for three stations with different snow classes are shown in Figures 2c and 2e, over a period of time that all stations were operational. However, the reported $p_{\rm ubs}$ is for the entire available data at each station.

At the Monahan flat in Alaska with perennial tundra snow and $p_{\rm ubs} = 0.38$, the seasonality of ST is not synchronous with the presence and absence of snow, especially after the calendar year 2012. During the late fall when the snow begins to deepen and late winter when it starts to melt, the ST changes gradually and there are transitioning time windows over which the ST is above the freezing point. The mean SD below which the soil is unfrozen is around 0.2 m; however, it can be seen that SD varies significantly, likely due to the snowfall climatology of the station.

For a deep seasonal alpine snow at the Big Flat station, with $p_{\rm ubs} = 0.64$, the dynamics of temperature and snow are synchronous. Unfrozen soil persists, with temperatures barely above 0°C, throughout the winter even when SD is greater than 2 m. The melting time is in order of a few weeks and the changes in seasonal snow significantly contribute to the increase of ST (Zhang, 2005). Over the time window of snow melting from more than 1 m to zero, STs sharply increases from 0 to more than 10°C. At the Bear river station with shallower and less persistent prairie snow, $p_{\rm ubs}$ is 0.88. The bottom ST is noticeably above the freezing point throughout the entire snow accumulation seasons, compared to the Big Flat station.

GAO ET AL. 5 of 12

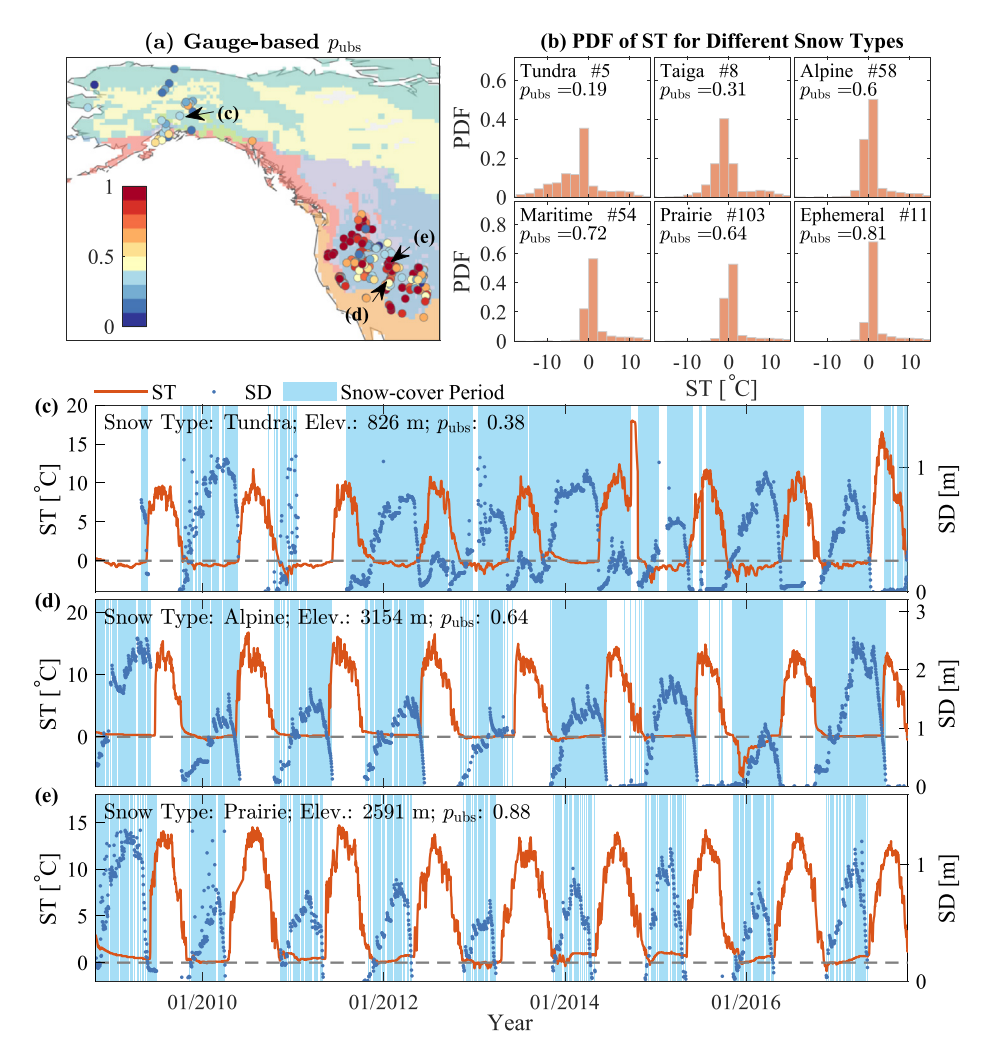


Figure 2. Annual probability of snowpack with unfrozen bottom soil $p_{\rm ubs}$ at selected SNOwpack TELemetry sites (a), probability density function (PDF) of bottom soil temperature (ST) for stations with the same snow type (b), and time series of ST and snow depth (SD) at the Monahan flat (63°2′N, 147°4′W) (c), Big Flat (38°18′N, 111°21′W) (d), and Bear River (40°5′N, 110°5′W) (e) stations. The number of stations used for demonstration of the PDFs and corresponding $p_{\rm ubs}$ are presented in the legends.

4.2. Seasonal Variability

Figures 3a–3c shows the mean seasonal evolution of SCE and SCE_{ubs} as well as their ratio. The data over Greenland is not considered as the MERRA-2 does not report the snow properties over the ice sheet. We observe that MERRA-2 (GLDAS) slightly overestimates (underestimates) ERA-Interim and ERA5 in terms of all three variables. While the seasonal evolution of all products are consistent, MERRA-2 exhibits the largest degree of uncertainty to the soil freezing threshold, especially during the late fall and winter.

Consistent with previous findings (Déry & Brown, 2007), SCE is minimum in July/August and begins to sharply increase from 1.4-2.4 million km² to its maximum 49-59 million km² in January. However, all reanalysis data consistently demonstrate that, unlike SCE, the extent of unfrozen bottom soil shows sub-annual bi-modality with two annual maxima in April and October. This pattern is due to a time lag between the rate of shrinkage/expansion of SCE and unfrozen soils. In fact, during the early melting seasons, when snow cover begins to decline from January to April, the retreating rate of SCE is slower than the expansion rate of unfrozen soils, leading to a notable increase of SCE_{ubs} . However, throughout the rest of melting seasons, the melting of snow accelerates and dominates the expanding rate of unfrozen soils. During the accumulation seasons, as snowfall becomes the dominant form of precipitation, the snow cover expands rapidly over warm soils until October. From October to

GAO ET AL. 6 of 12

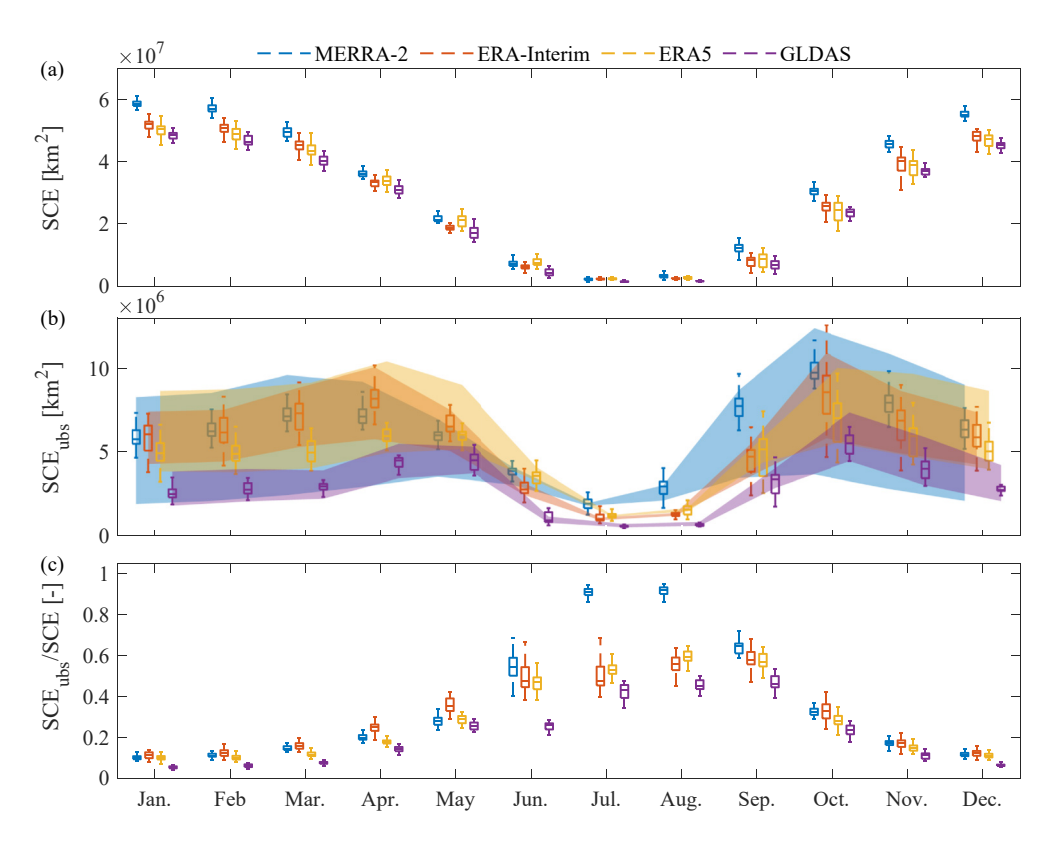


Figure 3. Seasonal evolution of snow cover extent (SCE) (a), SCE with unfrozen bottom soil (SCE_{ubs}) (b), and their ratio (c) in Northern Hemisphere excluding Greenland. The boxes show the 25th and 75th percentiles around the median and the whiskers extend to 1.5 times the interquartile. The shaded areas show the uncertainty when the freezing threshold is perturbed by $\pm 0.5^{\circ}$ C.

January, the frozen soil areas grow faster than SCE, resulting in a reduction of SCE_{ubs} . This bi-modality is largely controlled by the dynamics of snow cover and ST over Eurasia as shown in Figure 1, where the expansion and retraction of snow are more dramatic than over North America. Surprisingly, the ratio of SCE_{ubs} to SCE shows a seasonal cycle completely asynchronous with SCE (Figure 3c).

It is important to note that the presented results are based on the mean-cell values for all reanalysis products. Thus, when a snow fraction within a grid cell is less than 100%, the snow bottom ST could be overestimated, especially in ephemeral snow regions. This overestimation makes the results sensitive to SD uncertainties to some extent. To examine such sensitivity, we changed the SD thresholds from 0.1 to 5 cm (Figure S2, Supporting Information S1). The analyses show that the results can be quite sensitive to this threshold and increasing the threshold makes the values of SCE far less than other climate data records (Estilow et al., 2015; Mudryk et al., 2020). Nevertheless, we found that such uncertainty generally has limited influence on the observed seasonal evolution of SCE and SCE_{ubs} as well as their ratios.

4.3. Interannual Variability and Trends

It is well documented that SCE is declining in a warming climate (Brown, 2000; Déry & Brown, 2007; R. Brown & Derksen, 2013; Chen et al., 2016; Y. Zhang & Ma, 2018; Bormann et al., 2018; Mudryk et al., 2020). The question is whether melting of snowpack from the bottom has accelerated or not in the past few decades. Confining our considerations to MERRA-2, ERA-Interim, and ERA5, we quantify interannual variability of the monthly SCE and ratios of SCE across different latitudinal belts over the observation periods (see Table. 1). Throughout, the null hypothesis is that there exists no interannual trend and we reject it when the p-values are smaller than a significance level of 0.05.

GAO ET AL. 7 of 12



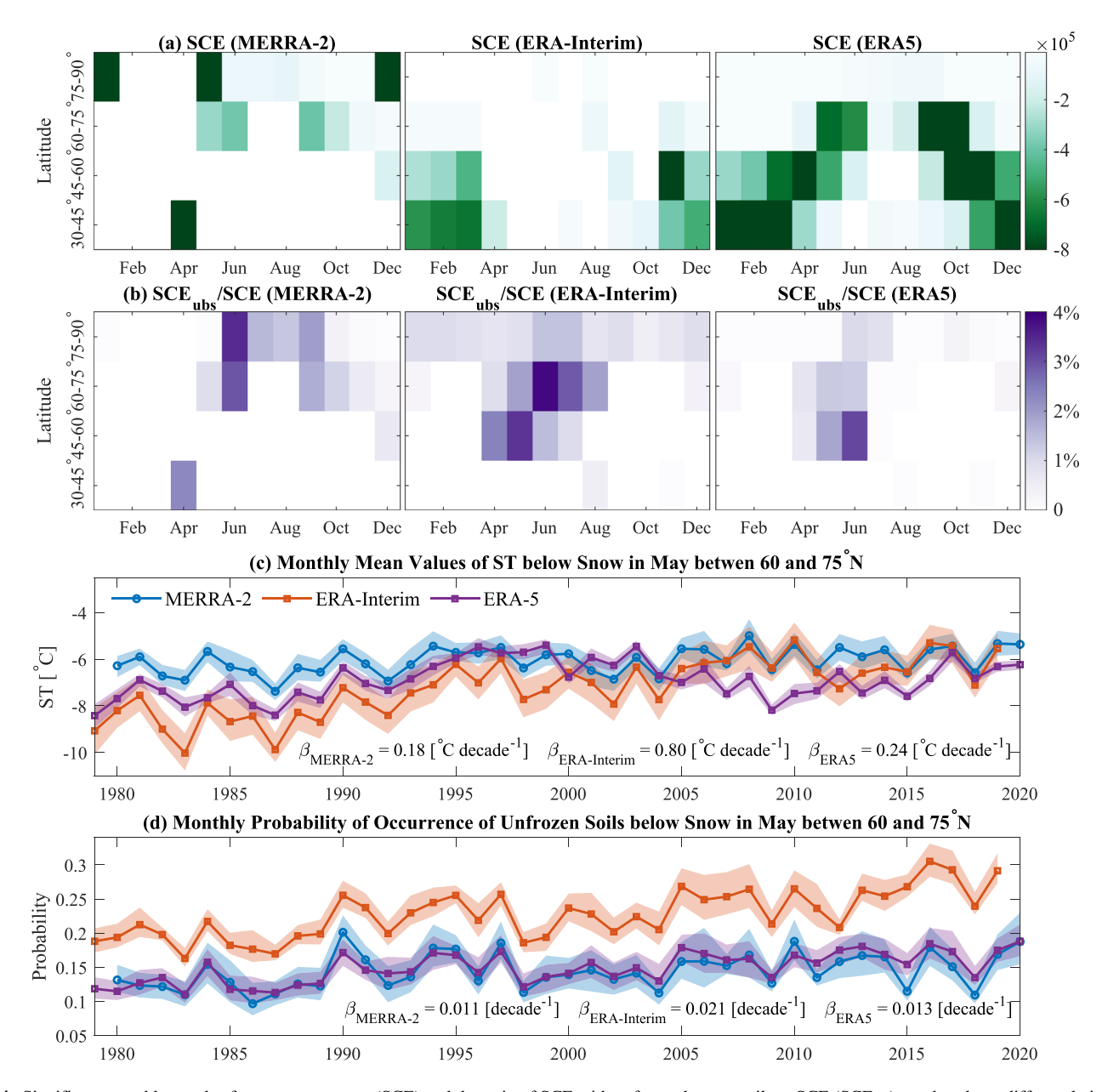


Figure 4. Significant monthly trends of snow cover extent (SCE) and the ratio of SCE with unfrozen bottom soils to SCE (SCE_{ubs}) per decade, at different latitudinal belts (a+b) as well as monthly mean values of hourly soil temperature (ST) (c) and occurrence of unfrozen soils below snowpack in month of May within $60 - 75^{\circ}$ N (d). Only significant trends (*p*-value <0.05) are shown and the shaded areas are 95% bootstrap percentiles, obtained based on daily mean values.

Consistent with previous findings, all reanalysis data (Figure 4a) demonstrate that the monthly mean SCE exhibits a significant declining trend across different seasons and latitudes, although there exist some notable inconsistencies in the magnitude, seasonality, and location. Unlike SCE, the monthly mean values of the ratio exhibit a significant positive trend in all three reanalysis data (Figure 4b)—mainly from early spring to early fall. In other words, the data indicate that expansion of unfrozen bottom soil could outpace shrinkage of SCE. Even though, the reanalysis data are not fully consistent in terms of the space-time distribution of the trends, it appears that throughout the year, significant values become more frequent over higher latitudes and reach to 3%–4% per decade. Note that uncertainty analysis, in response to changes of SD, indicates that SD thresholds have very limited influence on the trends of SCE and ratios of SCE_{ubs} to SCE.

Since the majority of positive trends are in spring, it appears that bottom melting could be a major contributing factor in reported shrinkage of springtime NH snowpack (Bormann et al., 2018; Derksen & Brown, 2012). For

GAO ET AL. 8 of 12



example, as shown in Figure 4c, the mean values of ST, below arctic snow $(60-75^{\circ})$ in spring, are warming up at the rate of 0.18 and 0.8°C per decade in ERA-Interim (ERA5) and MERRA-2, respectively. Even though, the mean values are below zero, as demonstrated in Figure 4d, this non-stationarity manifests itself in a growing probability of occurrence of unfrozen bottom soil with a rate of 0.011-0.021 per decade. Compared to 40 years ago, the taiga and tundra snow, above the Arctic Circle, are now experiencing 50% more unfrozen bottom soil in the month of May. Note that since 2004, ERA5 has assimilated snow-no-snow satellite data (Mortimer et al., 2020). Therefore, any changes of the trends in ST after 2004 and its possible connections with the effects of satellite snow data assimilation worth further investigations.

5. Summary and Concluding Remarks

Using snow depth and topmost soil temperature from MERRA-2, ERA-Interim, ERA5, and GLDAS reanalysis data as well as ground measurements from the SNOTEL network; this paper studied the spatiotemporal variability of snow cover extent with unfrozen bottom soil (SCE_{ubs}) at multiple scales and its interannual trend in Northern Hemisphere. It was documented that, on average, 30% of annual snow extent covers unfrozen soil, while during July and August, this ratio ranges from 45 (GLDAS) to 95% (MERRA-2). We demonstrated that unfrozen soil is more frequent below the ephemeral followed by the maritime and prairie snow. Seasonal analysis indicated that, unlike snow cover, SCE_{ubs} exhibits a sub-annual bi-modality and reaches its maximum in April and October. The trend analysis indicated that over middle to high latitudes $(45-75^{\circ})$, where the dominant snow types are taiga and tundra, expansion of unfrozen soils below snowpack has outpaced the shrinkage of snow cover extent - an indication of accelerated basal snowpack melting.

On the other hand, we observed noticeable differences amongst reanalysis products for both SCE and soil temperature. Future research is still needed to investigate the reasons about the observed differences for improved parameterization of the snowpack ground heat flux. Additionally, current satellite data do not provide any information about soil moisture below wet snowpack (Entekhabi et al., 2010; Kerr et al., 2010; Njoku et al., 2003). The results of this study show that unfrozen soil and thus liquid soil moisture below snowpack are widespread globally even during the winter. Future research is needed to understand how the presence of liquid soil moisture below snowpack can change its microwave emission and to develop algorithms for its global passive microwave retrievals.

Data Availability Statement

MERRA-2 data set are publicly available through http://doi.org/10.5067/RKPHT8KC1Y1T; ERA-Interim data set are available through https://apps.ecmwf.int/datasets/data/interim-full-daily/levtype=sfc/; ERA5 data set are available at http://doi.org/10.24381/cds.adbb2d47; GLDAS data set are available at http://doi.org/10.5067/ E7TYRXPJKWOQ.

References

Albergel, C., Dutra, E., Muñoz-Sabater, J., Haiden, T., Balsamo, G., Beljaars, A., & Wedi, N. (2015). Soil temperature at ECMWF: An assessment using ground-based observations. Journal of Geophysical Research: Atmospheres, 120(4), 1361-1373. https://doi.org/10.1002/2014jd022505 André, C., Ottlé, C., Royer, A., & Maignan, F. (2015). Land surface temperature retrieval over circumpolar arctic using ssm/i-ssmis and modis data. Remote Sensing of Environment, 162, 1-10. https://doi.org/10.1016/j.rse.2015.01.028

Barnett, T. P., Adam, J. C., & Lettenmaier, D. P. (2005). Potential impacts of a warming climate on water availability in snow-dominated regions. Nature, 438(7066), 303-309. https://doi.org/10.1038/nature04141

Barnhart, T. B., Molotch, N. P., Livneh, B., Harpold, A. A., Knowles, J. F., & Schneider, D. (2016). Snowmelt rate dictates streamflow. Geophysical Research Letters, 43(15), 8006-8016. https://doi.org/10.1002/2016g1069690

Blankinship, J. C., Meadows, M. W., Lucas, R. G., & Hart, S. C. (2014). Snowmelt timing alters shallow but not deep soil moisture in the sierra Nevada, Water Resources Research, 50(2), 1448–1456, https://doi.org/10.1002/2013wr014541

Boike, J., Roth, K., & Ippisch, O. (2003). Seasonal snow cover on frozen ground: Energy balance calculations of a permafrost site near ny-âlesund, Spitsbergen. Journal of Geophysical Research, 108(D2). https://doi.org/10.1029/2001jd000939

Bormann, K. J., Brown, R. D., Derksen, C., & Painter, T. H. (2018). Estimating snow-cover trends from space. Nature Climate Change, 8(11), 924-928. https://doi.org/10.1038/s41558-018-0318-3

Brown, R., & Derksen, C. (2013). Is eurasian october snow cover extent increasing? Environmental Research Letters, 8(2), 024006. https://doi. org/10.1088/1748-9326/8/2/024006

Brown, R. D. (2000). Northern hemisphere snow cover variability and change, 1915–97. Journal of Climate, 13(13), 2339–2355. https://doi. org/10.1175/1520-0442(2000)013<2339:nhscva>2.0.co;2

2145. https://doi.org/10.1175/2008jcli2665.1

ick-Jackson. L. Gao is also supported by the Heinz G. Stefan Fellowship and Doctoral Dissertation Fellowship from the University of Minnesota, J. Cohen is supported by the US National Science Foundation grants PLR-1901352. The authors also thank Dr. Chris Derksen at Environment and Climate Change Canada

for insightful discussion. The first author

also acknowledges technical support from Sagar Tamang at University of Minnesota

for trend analysis.

Acknowledgments

The authors highly acknowledge the support from the Future Investigators

in NASA Earth and Space Science (FINESST, 80NSSC19K1333) program

Remote Sensing Theory Program

through Dr Lucia Tsaoussi (RST. 80NSSC20K1717) Program as well as

the NASA's Interdisciplinary Science

(IDS, 80NSSC20K1294) program in

Earth Science through Dr. Gail Skofron-

through Dr. A. Leidner, and the NASA's

Brown, R. D., & Mote, P. W. (2009). The response of northern hemisphere snow cover to a changing climate, Journal of Climate, 22(8), 2124-

GAO ET AL. 9 of 12



- Brown, R. D., & Robinson, D. A. (2011). Northern hemisphere spring snow cover variability and change over 1922–2010 including an assessment of uncertainty. *The Cryosphere*, 5(1), 219–229. https://doi.org/10.5194/tc-5-219-2011
- Cao, B., Gruber, S., Zheng, D., & Li, X. (2020). The era5-land soil temperature bias in permafrost regions. *The Cryosphere*, 14(8), 2581–2595. https://doi.org/10.5194/tc-14-2581-2020
- Chen, X., Liang, S., & Cao, Y. (2016). Satellite observed changes in the northern hemisphere snow cover phenology and the associated radiative forcing and feedback between 1982 and 2013. *Environmental Research Letters*, 11(8), 084002. https://doi.org/10.1088/1748-9326/11/8/084002 Cohen, J. (1994). Snow cover and climate. *Weather*, 49(5), 150–156. https://doi.org/10.1002/j.1477-8696.1994.tb05997.x
- Cohen, J., & Rind, D. (1991). The effect of snow cover on the climate. *Journal of Climate*, 4(7), 689–706. https://doi.org/10.1175/1520-0442(1991)004<0689:teosco>2.0.co;2
- Cohen, J. L., Furtado, J. C., Barlow, M. A., Alexeev, V. A., & Cherry, J. E. (2012). Arctic warming, increasing snow cover and widespread boreal winter cooling. Environmental Research Letters, 7(1), 014007. https://doi.org/10.1088/1748-9326/7/1/014007
- Decker, K., Wang, D., Waite, C., & Scherbatskoy, T. (2003). Snow removal and ambient air temperature effects on forest soil temperatures in northern Vermont. Soil Science Society of America Journal, 67(4), 1234–1242. https://doi.org/10.2136/sssaj2003.1234
- Dee, D. P., Uppala, S. M., Simmons, A., Berrisford, P., Poli, P., Kobayashi, S., et al. (2011). The era-interim reanalysis: Configuration and performance of the data assimilation system. The Quarterly Journal of the Royal Meteorological Society, 137(656), 553–597. https://doi.org/10.1002/qj.828
- Derksen, C., & Brown, R. (2012). Spring snow cover extent reductions in the 2008–2012 period exceeding climate model projections. *Geophysical Research Letters*, 39(19). https://doi.org/10.1029/2012gl053387
- Déry, S. J., & Brown, R. D. (2007). Recent northern hemisphere snow cover extent trends and implications for the snow-albedo feedback. Geophysical Research Letters, 34(22). https://doi.org/10.1029/2007g1031474
- DeWalle, D. R., & Rango, A. (2008). Principles of snow hydrology. Cambridge University Press.
- Dominé, F., & Shepson, P. B. (2002). Air-snow interactions and atmospheric chemistry. Science, 297(5586), 1506–1510. https://doi.org/10.1126/science.1074610
- Dorigo, W., Wagner, W., Hohensinn, R., Hahn, S., Paulik, C., Xaver, A., et al. (2011). The international soil moisture network: A data hosting facility for global in situ soil moisture measurements. *Hydrology and Earth System Sciences*, 15(5), 1675–1698. https://doi.org/10.5194/hess-15-1675-2011
- Dorigo, W., Xaver, A., Vreugdenhil, M., Gruber, A., Hegyiova, A., Sanchis-Dufau, A., & Drusch, M. (2013). Global automated quality control of in situ soil moisture data from the international soil moisture network. *Vadose Zone Journal*, 12(3). https://doi.org/10.2136/vzj2012.0097
- Douglas, E., Vogel, R., & Kroll, C. (2000). Trends in floods and low flows in the United States: Impact of spatial correlation. *Journal of Hydrology*, 240(1–2), 90–105. https://doi.org/10.1016/s0022-1694(00)00336-x
- Duan, S.-B., Li, Z.-L., & Leng, P. (2017). A framework for the retrieval of all-weather land surface temperature at a high spatial resolution from polar-orbiting thermal infrared and passive microwave data. *Remote Sensing of Environment*, 195, 107–117. https://doi.org/10.1016/j.
- Earman, S., Campbell, A. R., Phillips, F. M., & Newman, B. D. (2006). Isotopic exchange between snow and atmospheric water vapor: Estimation of the snowmelt component of groundwater recharge in the southwestern United States. *Journal of Geophysical Research*, 111(D9). https://doi.org/10.1029/2005id006470
- Entekhabi, D., Njoku, E. G., O'Neill, P. E., Kellogg, K. H., Crow, W. T., Edelstein, W. N., et al. (2010). The soil moisture active passive (smap) mission. *Proceedings of the IEEE*, 98(5), 704–716.
- Estilow, T. W., Young, A. H., & Robinson, D. A. (2015). A long-term northern hemisphere snow cover extent data record for climate studies and monitoring. *Earth System Science Data*, 7(1), 137–142. https://doi.org/10.5194/essd-7-137-2015
- Gelaro, R., McCarty, W., Suárez, M. J., Todling, R., Molod, A., Takacs, L., et al. (2017). The modern-era retrospective analysis for research and applications, version 2 (merra-2). *Journal of Climate*, 30(14), 5419–5454. https://doi.org/10.1175/jcli-d-16-0758.1
- Goodrich, L. E. (1982). The influence of snow cover on the ground thermal regime. Canadian Geotechnical Journal, 19(4), 421–432. https://doi.org/10.1139/t82-047
- Granger, R., & Male, D. (1978). Melting of a prairie snowpack. *Journal of Applied Meteorology and Climatology*, 17(12), 1833–1842. https://doi.org/10.1175/1520-0450(1978)017<1833:moaps>2.0.co;2
- Gray, D. M. (1970). Handbook on the principles of hydrology.
- Hersbach, H., Bell, B., Berrisford, P., Hirahara, S., Horányi, A., Muñoz-Sabater, J., et al. (2020). The era5 global reanalysis. *Quarterly Journal of the Royal Meteorological Society*, 146(730), 1999–2049. https://doi.org/10.1002/qj.3803
- Holmes, T., De Jeu, R., Owe, M., & Dolman, A. (2009). Land surface temperature from ka band (37 ghz) passive microwave observations. *Journal of Geophysical Research*, 114(D4). https://doi.org/10.1029/2008jd010257
- Holmes, T., Jackson, T. J., Reichle, R. H., & Basara, J. B. (2012). An assessment of surface soil temperature products from numerical weather prediction models using ground-based measurements. *Water Resources Research*, 48(2). https://doi.org/10.1029/2011wr010538
- Huang, Y., Jiang, J., Ma, S., Ricciuto, D., Hanson, P. J., & Luo, Y. (2017). Soil thermal dynamics, snow cover, and frozen depth under five temperature treatments in an ombrotrophic bog: Constrained forecast with data assimilation. *Journal of Geophysical Research: Biogeosciences*, 122(8), 2046–2063. https://doi.org/10.1002/2016jg003725
- Iwata, Y., Hayashi, M., Suzuki, S., Hirota, T., & Hasegawa, S. (2010). Effects of snow cover on soil freezing, water movement, and snowmelt infiltration: A paired plot experiment. Water Resources Research, 46(9). https://doi.org/10.1029/2009wr008070
- Jiménez-Muñoz, J. C., Sobrino, J. A., Skoković, D., Mattar, C., & Cristóbal, J. (2014). Land surface temperature retrieval methods from landsat-8 thermal infrared sensor data. IEEE Geoscience and Remote Sensing Letters, 11(10), 1840–1843. https://doi.org/10.1109/lgrs.2014.2312032
- Karl, T. R., Groisman, P. Y., Knight, R. W., & Heim, R. R., Jr. (1993). Recent variations of snow cover and snowfall in North America and their relation to precipitation and temperature variations. *Journal of Climate*, 6(7), 1327–1344. https://doi. org/10.1175/1520-0442(1993)006<1327;rvosca>2.0.co:2
- Kerr, Y. H., Lagouarde, J. P., & Imbernon, J. (1992). Accurate land surface temperature retrieval from avhrr data with use of an improved split window algorithm. Remote Sensing of Environment, 41(2–3), 197–209. https://doi.org/10.1016/0034-4257(92)90078-x
- Kerr, Y. H., Waldteufel, P., Wigneron, J.-P., Delwart, S., Cabot, F., Boutin, J., et al. (2010). othersThe smos mission: New tool for monitoring key elements of the global water cycle. *Proceedings of the IEEE*, 98(5), 666–687. https://doi.org/10.1109/jproc.2010.2043032
- Lemke, P., Ren, J., Alley, R. B., Allison, I., Carrasco, J., Flato, G., et al. (2007). Observations: Changes in snow, ice and frozen ground.
- Mankin, J. S., Viviroli, D., Singh, D., Hoekstra, A. Y., & Diffenbaugh, N. S. (2015). The potential for snow to supply human water demand in the present and future. *Environmental Research Letters*, 10(11), 114016. https://doi.org/10.1088/1748-9326/10/11/114016
- Mao, K., Qin, Z., Shi, J., & Gong, P. (2005). A practical split-window algorithm for retrieving land-surface temperature from modis data. *International Journal of Remote Sensing*, 26(15), 3181–3204. https://doi.org/10.1080/01431160500044713

GAO ET AL. 10 of 12



- Marks, D., & Winstral, A. (2001). Comparison of snow deposition, the snow cover energy balance, and snowmelt at two sites in a semiarid mountain basin. *Journal of Hydrometeorology*, 2(3), 213–227. https://doi.org/10.1175/1525-7541(2001)002<0213:cosdts>2.0.co;2
- Matoušek, J., Mount, D. M., & Netanyahu, N. S. (1998). Efficient randomized algorithms for the repeated median line estimator. *Algorithmica*, 20(2), 136–150.
- Mazurkiewicz, A. B., Callery, D. G., & McDonnell, J. J. (2008). Assessing the controls of the snow energy balance and water available for runoff in a rain-on-snow environment. *Journal of Hydrology*, 354(1–4), 1–14. https://doi.org/10.1016/j.jhydrol.2007.12.027
- McCabe, G. J., & Wolock, D. M. (2010). Long-term variability in northern hemisphere snow cover and associations with warmer winters. Climatic Change, 99(1), 141–153. https://doi.org/10.1007/s10584-009-9675-2
- McFarland, M. J., Miller, R. L., & Neale, C. M. (1990). Land surface temperature derived from the ssm/i passive microwave brightness temperatures. IEEE Transactions on Geoscience and Remote Sensing, 28(5), 839–845. https://doi.org/10.1109/36.58971
- Mortimer, C., Mudryk, L., Derksen, C., Luojus, K., Brown, R., Kelly, R., & Tedesco, M. (2020). Evaluation of long-term northern hemisphere snow water equivalent products. The Cryosphere, 14(5), 1579–1594. https://doi.org/10.5194/tc-14-1579-2020
- Mudryk, L., Kushner, P., Derksen, C., & Thackeray, C. (2017). Snow cover response to temperature in observational and climate model ensembles. Geophysical Research Letters, 44(2), 919–926. https://doi.org/10.1002/2016gl071789
- Mudryk, L., Santolaria-Otín, M., Krinner, G., Ménégoz, M., Derksen, C., Brutel-Vuilmet, C., & Essery, R. (2020). Historical northern hemisphere snow cover trends and projected changes in the cmip6 multi-model ensemble. The Cryosphere, 14(7), 2495–2514. https://doi.org/10.5194/ tc-14-2495-2020
- Nijssen, B., O'Donnell, G. M., Hamlet, A. F., & Lettenmaier, D. P. (2001). Hydrologic sensitivity of global rivers to climate change. Climatic Change, 50(1), 143–175. https://doi.org/10.1023/a:1010616428763
- Njoku, E. G., Jackson, T. J., Lakshmi, V., Chan, T. K., & Nghiem, S. V. (2003). Soil moisture retrieval from amsr-e. *IEEE Transactions on Geoscience and Remote Sensing*, 41(2), 215–229. https://doi.org/10.1109/tgrs.2002.808243
- Njoku, E. G., & Li, L. (1999). Retrieval of land surface parameters using passive microwave measurements at 6-18 ghz. *IEEE Transactions on Geoscience and Remote Sensing*, 37(1), 79–93. https://doi.org/10.1109/36.739125
- Pomeroy, J., & Brun, E. (2001). Physical properties of snow. Snow ecology: An interdisciplinary examination of snow-covered ecosystems, 45,
- Pomeroy, J., Toth, B., Granger, R., Hedstrom, N., & Essery, R. (2003). Variation in surface energetics during snowmelt in a subarctic mountain catchment. *Journal of Hydrometeorology*, 4(4), 702–719. https://doi.org/10.1175/1525-7541(2003)004<0702:viseds>2.0.co;2
- Pulliainen, J., Aurela, M., Laurila, T., Aalto, T., Takala, M., Salminen, M., et al. (2017). Early snowmelt significantly enhances boreal springtime carbon uptake. *Proceedings of the National Academy of Sciences*, 114(42), 11081–11086. https://doi.org/10.1073/pnas.1707889114
- Reichle, R. H., Draper, C. S., Liu, Q., Girotto, M., Mahanama, S. P., Koster, R. D., & De Lannoy, G. J. (2017). Assessment of merra-2 land surface
- hydrology estimates. *Journal of Climate*, 30(8), 2937–2960. https://doi.org/10.1175/jcli-d-16-0720.1 Robinson, D. A., Dewey, K. F., & Heim, R. R., Jr. (1993). Global snow cover monitoring: An update. *Bulletin of the American Meteorological*
- Society, 74(9), 1689–1696. https://doi.org/10.1175/1520-0477(1993)074<1689:gscmau>2.0.co;2
 Rodell, M., Houser, P., Jambor, U., Gottschalck, J., Mitchell, K., Meng, C.-J., et al. (2004). The global land data assimilation system. Bulletin of
- the American Meteorological Society, 85(3), 381–394. https://doi.org/10.1175/bams-85-3-381
 Schaefer, G. L., & Paetzold, R. F. (2001). Snotel (snowpack telemetry) and scan (soil climate analysis network). In Automated weather stations for
- applications in agriculture and water resources management: Current use and future perspectives (Vol. 1074, pp. 187–194). Sen, P. K. (1968). Estimates of the regression coefficient based on kendall's tau. Journal of the American Statistical Association, 63(324),
- 1379–1389. https://doi.org/10.1080/01621459.1968.10480934
- Serreze, M. C., Clark, M. P., Armstrong, R. L., McGinnis, D. A., & Pulwarty, R. S. (1999). Characteristics of the western United States snowpack from snowpack telemetry (snotel) data. Water Resources Research, 35(7), 2145–2160. https://doi.org/10.1029/1999wr900090
- Sobrino, J. A., Jiménez-Muñoz, J. C., & Paolini, L. (2004). Land surface temperature retrieval from landsat tm 5. Remote Sensing of Environment, 90(4), 434–440. https://doi.org/10.1016/j.rse.2004.02.003
- Sturm, M., Holmgren, J., & Liston, G. E. (1995). A seasonal snow cover classification system for local to global applications. *Journal of Climate*, 8(5), 1261–1283. https://doi.org/10.1175/1520-0442(1995)008<1261;assccs>2.0.co;2
- Tamang, S. K., Ebtehaj, A. M., Prein, A. F., & Heymsfield, A. J. (2020). Linking global changes of snowfall and wet-bulb temperature. *Journal of Climate*, 33(1), 39–59. https://doi.org/10.1175/jcli-d-19-0254.1
- Theil, H. (1992). A rank-invariant method of linear and polynomial regression analysis. In *Henri theil's contributions to economics and econometrics* (pp. 345–381). Springer, https://doi.org/10.1007/078.04.011.2546.8.20
- metrics (pp. 345–381). Springer. https://doi.org/10.1007/978-94-011-2546-8_20
 Toure, A. M., Reichle, R. H., Forman, B. A., Getirana, A., & De Lannoy, G. J. (2018). Assimilation of modis snow cover fraction observations
- into the NASA catchment land surface model. *Remote Sensing*, 10(2), 316. https://doi.org/10.3390/rs10020316

 Tyler, S. W., Burak, S. A., McNamara, J. P., Lamontagne, A., Selker, J. S., & Dozier, J. (2008). Spatially distributed temperatures at the base of two mountain snowpacks measured with fiber-optic sensors. *Journal of Glaciology*, 54(187), 673–679. https://doi.org/10.3189/002214308786570827
- Vavrus, S. (2007). The role of terrestrial snow cover in the climate system. Climate Dynamics, 29(1), 73-88. https://doi.org/10.1007/s00382-007-0226-0
- Wang, L., Li, X., Chen, Y., Yang, K., Chen, D., Zhou, J., & Huang, J. (2016). Validation of the global land data assimilation system based on measurements of soil temperature profiles. *Agricultural and Forest Meteorology*, 218, 288–297. https://doi.org/10.1016/j.agrformet.2016.01.003
- Wilcox, R. R. (2010). Fundamentals of modern statistical methods: Substantially improving power and accuracy. Springer.
- Williams, P. J., & Smith, M. W. (1991). The frozen earth (Tech. Rep.). Cambridge University Press.
- Winchell, T. S., Barnard, D. M., Monson, R. K., Burns, S. P., & Molotch, N. P. (2016). Earlier snowmelt reduces atmospheric carbon uptake in midlatitude subalpine forests. *Geophysical Research Letters*, 43(15), 8160–8168. https://doi.org/10.1002/2016gl069769
- Wu, W.-Y., Lo, M.-H., Wada, Y., Famiglietti, J. S., Reager, J. T., Yeh, P. J.-F., & Yang, Z.-L. (2020). Divergent effects of climate change on future groundwater availability in key mid-latitude aquifers. *Nature Communications*, 11(1), 1–9. https://doi.org/10.1038/s41467-020-17581-y
- Yang, K., & Zhang, J. (2018). Evaluation of reanalysis datasets against observational soil temperature data over China. *Climate Dynamics*, 50(1), 317–337, https://doi.org/10.1007/s00382-017-3610-4
- Yue, S., & Pilon, P. (2004). A comparison of the power of the t test, mann-kendall and bootstrap tests for trend detection/une comparaison de la puissance des tests t de student, de mann-kendall et du bootstrap pour la détection de tendance. *Hydrological Sciences Journal*, 49(1), 21–37. https://doi.org/10.1623/hysj.49.1.21.53996
- Zhang, T. (2005). Influence of the seasonal snow cover on the ground thermal regime: An overview. Reviews of Geophysics, 43(4). https://doi.org/10.1029/2004rg000157
- Zhang, Y., & Ma, N. (2018). Spatiotemporal variability of snow cover and snow water equivalent in the last three decades over Eurasia. *Journal of Hydrology*, 559, 238–251. https://doi.org/10.1016/j.jhydrol.2018.02.031

GAO ET AL. 11 of 12



- Zhao, L., Gray, D. M., & Male, D. H. (1997). Numerical analysis of simultaneous heat and mass transfer during infiltration into frozen ground. Journal of Hydrology, 200(1–4), 345–363. https://doi.org/10.1016/s0022-1694(97)00028-0
- Zhu, L., Ives, A. R., Zhang, C., Guo, Y., & Radeloff, V. C. (2019). Climate change causes functionally colder winters for snow cover-dependent organisms. Nature Climate Change, 9(11), 886–893. https://doi.org/10.1038/s41558-019-0588-4
- Zona, D., Gioli, B., Commane, R., Lindaas, J., Wofsy, S. C., Miller, C. E., et al. (2016). Cold season emissions dominate the arctic tundra methane budget. Proceedings of the National Academy of Sciences, 113(1), 40–45. https://doi.org/10.1073/pnas.1516017113

References From the Supporting Information

- Albergel, C., Balsamo, G., Rosnay, P. d., Muñoz-Sabater, J., & Boussetta, S. (2012). A bare ground evaporation revision in the ECMWF land-surface scheme: Evaluation of its impact using ground soil moisture and satellite microwave data. *Hydrology and Earth System Sciences*, 16(10), 3607–3620. https://doi.org/10.5194/hess-16-3607-2012
- Albergel, C., Dutra, E., Munier, S., Calvet, J.-C., Munoz-Sabater, J., Rosnay, P. d., & Balsamo, G. (2018). Era-5 and era-interim driven isba land surface model simulations: Which one performs better? *Hydrology and Earth System Sciences*, 22(6), 3515–3532. https://doi.org/10.5194/hess-22-3515-2018
- Anderson, E. A. (1976). A point energy and mass balance model of a snow cover. Stanford University.
- Balsamo, G., Beljaars, A., Scipal, K., Viterbo, P., van den Hurk, B., Hirschi, M., & Betts, A. K. (2009). A revised hydrology for the ECMWF model: Verification from field site to terrestrial water storage and impact in the integrated forecast system. *Journal of Hydrometeorology*, 10(3), 623–643. https://doi.org/10.1175/2008jhm1068.1
- Balsamo, G., Boussetta, S., Dutra, E., Beljaars, A., Viterbo, P., & Van den Hurk, B. (2011). Evolution of land surface processes in the ifs. ECMWF newsletter, 127(17–22), 78.
- Barry, R., Prévost, M., Stein, J., & Plamondon, A. P. (1990). Application of a snow cover energy and mass balance model in a balsam fir forest. Water Resources Research, 26(5), 1079–1092, https://doi.org/10.1029/wr026i005p01079
- Boone, A., & Etchevers, P. (2001). An intercomparison of three snow schemes of varying complexity coupled to the same land surface model: Local-scale evaluation at an alpine site. *Journal of Hydrometeorology*, 2(4), 374–394. https://doi.org/10.1175/1525-7541(2001)002<0374:aiot ss>2.0.co:2
- Boussetta, S., Balsamo, G., Beljaars, A., Kral, T., & Jarlan, L. (2013). Impact of a satellite-derived leaf area index monthly climatology in a global numerical weather prediction model. *International Journal of Remote Sensing*, 34(9–10). 3520–3542. https://doi.org/10.1080/014311 61.2012.716543
- Douville, H., Royer, J.-F., & Mahfouf, J.-F. (1996). A new snow parameterization for the mto-France climate model part II: Validation in a 3-d gcm experiment. *Climate Dynamics*. *I*(12), 37–52.
- Dutra, E., Balsamo, G., Viterbo, P., Miranda, P., Beljaars, A., Schär, C., & Elder, K. (2009). New snow scheme in htessel: Description and offline validation. ECMWF.
- Dutra, E., Balsamo, G., Viterbo, P., Miranda, P. M., Beljaars, A., Schär, C., & Elder, K. (2010). An improved snow scheme for the ECMWF land surface model: Description and offline validation. *Journal of Hydrometeorology*, 11(4), 899–916. https://doi.org/10.1175/2010jhm1249.1
- Hall, D., Salomonson, V., & Riggs, G. (2016). Modis/terra snow cover daily 13 global 0.058 cmg, version 5. NASA National Snow and Ice Data Center Distributed Active Archive Center, accessed 1.
- Koren, V., Schaake, J., Mitchell, K., Duan, Q.-Y., Chen, F., & Baker, J. (1999). A parameterization of snowpack and frozen ground intended for ncep weather and climate models. *Journal of Geophysical Research*, 104(D16), 19569–19585. https://doi.org/10.1029/1999jd900232
- Koster, R. D., Suarez, M. J., Ducharne, A., Stieglitz, M., & Kumar, P. (2000). A catchment-based approach to modeling land surface processes in a general circulation model: 1. Model structure. *Journal of Geophysical Research*, 105(D20), 24809–24822. https://doi. org/10.1029/2000jd900327
- Liu, R. Y., & Singh, K. (1992). Moving blocks jackknife and bootstrap capture weak dependence. *Exploring the Limits of Bootstrap*, 225, 248. Lynch-Stieglitz, M. (1994). The development and validation of a simple snow model for the giss gcm. *Journal of Climate*, 7(12), 1842–1855. https://doi.org/10.1175/1520-0442(1994)007<1842:tdayoa>2.0.co:2
- Mahrt, L., & Pan, H. (1984). A two-layer model of soil hydrology. Boundary-Layer Meteorology, 29(1), 1–20. https://doi.org/10.1007/bf00119116
 Niu, G.-Y., & Yang, Z.-L. (2006). Effects of frozen soil on snowmelt runoff and soil water storage at a continental scale. Journal of Hydrometeorology, 7(5), 937–952. https://doi.org/10.1175/jhm538.1
- Niu, G.-Y., Yang, Z.-L., Mitchell, K. E., Chen, F., Ek, M. B., Barlage, M., et al. (2011). The community noah land surface model with multiparameterization options (noah-mp): 1. Model description and evaluation with local-scale measurements. *Journal of Geophysical Research*, 116(D12). https://doi.org/10.1029/2010jd015139
- Noilhan, J., & Planton, S. (1989). A simple parameterization of land surface processes for meteorological models. *Monthly Weather Review*, 117(3), 536–549. https://doi.org/10.1175/1520-0493(1989)117<0536:aspols>2.0.co;2
- Schaake, J. C., Koren, V. I., Duan, Q.-Y., Mitchell, K., & Chen, F. (1996). Simple water balance model for estimating runoff at different spatial and temporal scales. *Journal of Geophysical Research*, 101(D3), 7461–7475. https://doi.org/10.1029/95jd02892
- Stieglitz, M., Ducharne, A., Koster, R., & Suarez, M. (2001). The impact of detailed snow physics on the simulation of snow cover and subsurface thermodynamics at continental scales. *Journal of Hydrometeorology*, 2(3), 228–242. https://doi.org/10.1175/1525-7541(2001)002<0228:tiodsp>2.0.co;2
- $van\ den\ Hurk,\ B.\ J.,\ Viterbo,\ P.,\ Beljaars,\ A.,\ \&\ Betts,\ A.\ (2000).\ \textit{Offline\ validation\ of\ the\ era 40\ surface\ scheme}.$
- Von Storch, H. (1995). Misuses of statistical analysis in climate. Analysis of Climate Variability: Applications of Statistical Techniques, 11–26. https://doi.org/10.1007/978-3-662-03744-7
- Yamazaki, T., & Kondo, J. (1992). The snowmelt and heat balance in snow-covered forested areas. Journal of Applied Meteorology and Climatology, 31(11), 1322–1327. https://doi.org/10.1175/1520-0450(1992)031<1322:tsahbi>2.0.co;2
- Yang, Z.-L., & Niu, G.-Y. (2003). The versatile integrator of surface and atmosphere processes: Part 1. Model description. Global and Planetary Change, 38(1–2), 175–189. https://doi.org/10.1016/s0921-8181(03)00028-6

GAO ET AL. 12 of 12